

Change in Fiber Properties Due to the Heat Treatment of Nylon 6 Tire Cords

J. P. Rath, T. K. Chaki, D. Khastgir

Rubber Technology Centre, Indian Institute of Technology, Kharagpur 721302, India

Received 17 July 2007; accepted 25 November 2007

DOI 10.1002/app.27941

Published online 17 March 2008 in Wiley InterScience (www.interscience.wiley.com).

ABSTRACT: Nylon 6 is used as a reinforcing material in different rubber products. However, as it is a thermoplastic material, it may undergo some kind of thermal shrinkage during the vulcanization of rubber, which leads to dimensional stability problems in the rubber product. To prevent this, we subjected nylon 6 to some kind of thermal treatment at higher temperatures. During thermal

treatment, there was some change in the mechanical properties, shrinkage which may have been correlated with changes in the crystal structure of the polymer. © 2008 Wiley Periodicals, Inc. *J Appl Polym Sci* 108: 3960–3967, 2008

Key words: nylon; strain; stress; X-ray

INTRODUCTION

In most industrial and consumer rubber products, textiles are used as the main backbone; they provide strength and dimensional stability. Mostly, polyester, nylon 66, and nylon 6 cords are used in rubber products. The intrinsic properties of a fiber are determined by its molecular structure–crystallinity, crystal structure, and degree of orientation rigidity of the molecular chains and intermolecular forces.¹ In tires, the reinforcements take the major share of the structural load of a vehicle. To obtain better performance and durability from a tire, the reinforcing elements should exhibit good strength, fatigue resistance, excellent toughness, low heat generation, and dimensional stability.^{2–10} Nylon tire cords have been used to make heavy-duty tires because of their high strength and good impact and fatigue resistance coupled with cost effectiveness. However, the overall performance of the tire is affected after its continuous operation. During actual running, the temperature of the tire increases because of frictional forces, hysteresis losses, and viscoelasticity and may reach as high as 150–160°C.⁴ In addition, during rubber product manufacturing, the cords may be exposed to a vulcanization temperature around 150°C. This adversely affects the dimensional stability as thermoplastic cords, such as nylon and polyester, undergo shrinkage when they are exposed to high temperatures.^{11,12} If no load is applied, the shrinkage is very high. So, often these cord materials are subjected to

heat treatment at much higher temperatures so that residual shrinkage at operating temperatures will be reduced. The effects of heat settings on the physical properties, dye uptake, viscoelastic behavior, and so on of nylon 6 have been reported in literature.^{13–18} The crystal structure of nylon 6 fibers and the characterization and modeling of different crystalline forms observed either because of manufacturing procedures or any after treatments have drawn much attention.^{19–25}

This investigation dealt with the study of the effect of thermal treatment on different properties of nylon 6 tire cords. The heat treatment was carried out at different temperatures ranging from 150 to 210°C for different durations. The residual shrinkage was then measured at 150°C. During the heat treatment under different temperatures, the tire cords were allowed to shrink freely and relax under controlled stress, which led to shrinkage when the applied stress was less than the shrinkage force and extension during thermal treatment when the applied stress was more than the shrinkage force.

The effect of heat treatment on the mechanical properties was also studied. The changes in mechanical properties were interpreted with help of changes in the crystalline structure of the fibers, as calculated from X-ray diffraction (XRD) and differential scanning calorimetry (DSC) studies.

EXPERIMENTAL

Double-ply greige (undipped) nylon 6 tire cords were obtained through Birla Tyres (Chhanpur, India) from their commercial supplier. The greige tire cords had a

Correspondence to: D. Khastgir (khasdi@rtc.iitkgp.ernet.in).

fineness of 1680/2 denier and a twist of 327–343 (turns per meter (TPM)).

The samples are designated either as NX, where X is the heat-treatment temperature without any load, or NXa, NXb, or NXc, where X represents the heat-setting temperature, a stands for the case when the applied force was less than the shrinkage force, b stands for the case when the applied load was equal to the shrinkage force, and c stands for the case when the applied force was higher than the shrinkage force. N0 stands for untreated cord.

Shrinkage

Shrinkage force and degree of shrinkage was measured with a thermal shrinkage testing machine (S. C. Dey & Co., Kolkata, India) at different temperatures (150, 170, 190, and 210°C). After we determined the shrinkage force at the aforementioned temperatures, shrinkage measurement was carried out at the same temperatures without and with different loads for 2 min. For free-shrinkage measurement, the pre-tension used was 0.001 g/denier. In the case of shrinkage measurement under a load, samples were quenched to room temperature under the same load.

XRD

XRD studies were carried out on a Philips PW 1729 X-ray generator with Ni-filtered Cu radiation under a 40-kV voltage and 30-mA current.

DSC

The DSC studies of the greige cords were performed on a TA Instruments (New Castle, DE) DSC-2920 under a nitrogen atmosphere at a heating rate of 10°C/min. The heat of fusion calculated from the melting endothermic peaks (ΔH) was used to calculate the crystallinities of the cords (ASTM E 974) with the following equation:²⁶

$$X_{\text{thermal}}(\%) = (\Delta H / \Delta H_0) \times 100 \quad (1)$$

where X_{thermal} is crystallinity determined from thermal analysis (DSC) and ΔH_0 is the heat of fusion for pure nylon 6 crystals (191 J/g).²⁷

Tensile properties

The tensile properties of cords were measured on a Hounsfield (KS-10) universal testing machine at 25°C with a gauge length of 150 mm and a crosshead speed of 200 mm/min. An average of five test results are reported, as per ASTM D 85.

RESULTS AND DISCUSSION

Thermal shrinkage

During manufacturing, polymeric fibers are formed into molecular structures with highly oriented chains in the fiber direction. This is accomplished through a series of thermomechanical processes. A high crystalline content is also achieved within the fiber.¹ Although polymeric fibers are highly oriented and crystallized, amorphous regions still exist in the yarns, and these regions significantly influence the cord's material properties. The amorphous region determines the glass-transition temperature of the fiber. Thermoplastic cords such as nylon and polyester, when subjected to high temperatures, exhibit some tendency to shrink.²⁸ This is because polymer chains in a fiber yarn are highly crystalline and oriented, and the orientation is in the direction of the fiber axis, which makes the fiber anisotropic in nature. However, this state of the fiber is a state of low entropy.²⁹ So whenever yarns are subjected to thermal treatment, the tendency will be for the fiber to go toward the state of higher entropy, and this is the reason for fiber shrinkage due to thermal disturbance during heat treatment.

The thermal force acts against the intermolecular force of attraction and holds the oriented polymer molecules present in the fiber. The magnitude of this force is substantially higher in the fiber form of the polymer compared to that in the ordinary polymer form. With increasing heat-treatment temperature, the shrinkage force increases for a fixed time of exposure. The variation of shrinkage force against exposure time at different temperatures, where thermal treatments were carried out, is presented in Figure 1. As also shown in this figure, at all temperatures of thermal treatment, initially, the shrinkage force increased with exposure time almost linearly and then

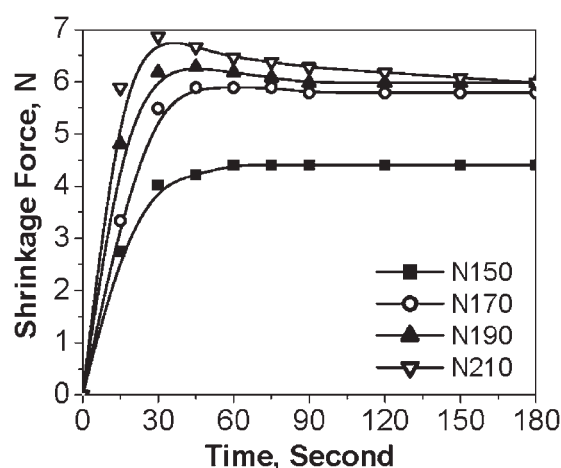


Figure 1 Shrinkage force versus time at different temperatures.

attained a plateau value within 30–50 s. However, at very high temperatures ($\geq 170^\circ\text{C}$) of exposure, a small drop in shrinkage force beyond 30–50 s was observed. This drop in shrinkage force may have been due to some kind of thermal softening of the fiber structure at elevated temperatures, and this effect became more pronounced when the exposure temperature was nearer to the melting point of the fiber.

Mostly, the shrinkage process was complete within 90 s; that is, 95% of the total shrinkage took place within 90 s. At all temperatures of thermal treatment, the free shrinkage of a cord increased with the exposure time, initially at a faster rate, and then assumed a steady-state value on prolonged exposure. The free shrinkage also increased with heat-treatment temperature at any particular time of exposure (Fig. 2).

However, when shrinkage was carried out under controlled conditions; that is, when the cords were exposed to heat treatment at different temperatures under some applied load, depending on the situation, there may have been expansion (when the applied stress was greater than the shrinkage stress) or contraction (when the applied stress was less than the shrinkage stress). These two situations are known as *heat setting* and *relaxation*.³⁰ So depending on the exposure temperature, the shrinkage force varied, as shown in Figure 1, and the applied stress at different temperatures had to be adjusted accordingly to get the heat setting and relaxation situation as required. The effects of different applied stresses at different thermal treatment temperatures are presented in Table I. When the applied stress is less than the shrinkage force, the amount of shrinkage increased with any particular temperature, initially at faster rate, and then slowly against the exposure time and with increasing load (within the shrinkage force), the degree of shrinkage always decreased. However, with increasing applied stress beyond the shrinkage stress at any temperature, there was an

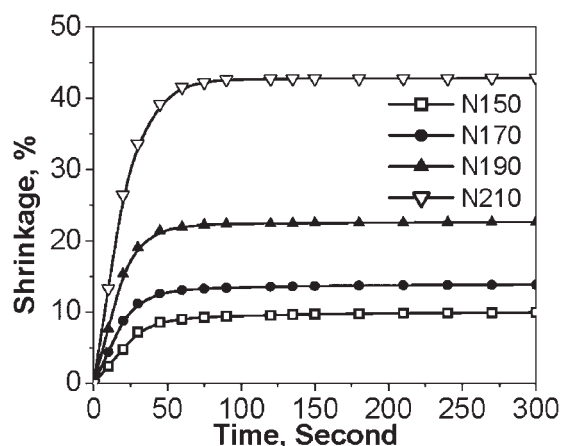


Figure 2 Shrinkage versus time at different temperatures.

TABLE I
Shrinkage at Different Loads and Temperatures

Temperature ($^\circ\text{C}$)	Load (N)	Shrinkage at different times (%)			
		30 s	60 s	120 s	300 s
150	2.95	3.60	4.74	4.86	4.96
	4.40	0.10	0.16	0.18	0.18
	5.90	-1.24	-1.86	-2.34	-2.46
	8.80	-3.17	-4.37	-4.46	-4.52
170	2.95	4.16	5.74	6.86	6.94
	4.40	2.62	3.72	3.88	3.96
	5.90	0.68	0.72	0.74	0.74
	8.80	-2.84	-3.78	-3.94	-4.04
190	2.95	4.74	5.98	6.34	6.42
	4.40	3.88	4.96	5.12	5.16
	6.27	0.42	0.54	0.56	0.56
	8.80	-2.02	-3.04	-3.24	-3.36
210	2.95	7.24	12.66	14.82	14.94
	4.40	5.82	9.26	10.12	10.22
	6.86	0.48	0.76	0.78	0.78
	8.80	-1.74	-2.66	-2.88	-2.94

Negative shrinkage represents expansion.

overall expansion of the cord that was expressed as negative shrinkage. This expansion increased when the applied stress increased further beyond the shrinkage force at any temperature of heat treatment. This expansion (negative shrinkage) was found to decrease with increasing exposure temperatures at a fixed load and to increase with time of exposure at a fixed temperature (Table I). That is, when the difference between shrinkage force and the applied stress decreased, the degree of shrinkage decreased.

Stress-strain properties

The stress-strain plots of nylon cords subjected to different conditions of heat treatment are presented in Figures 3–6 and Table II. The effect of the heat-treatment temperatures of the cords (under free-shrinkage conditions) is presented in Figure 3(a). With increasing temperature, the tenacity of the cord decreased, but there was an increase in the elongation at break with decreasing initial modulus. This was due to chain folding during heat treatment.³¹ However, at the highest temperature of treatment, which was 210°C , there was a drastic drop in both the tenacity and elongation at break [Fig. 3(b)]. This was because, during heat treatment, there was some internal change in the crystal structure of the cord, and the degree of change depended on the heat-treatment temperature.³² Perhaps this change was much higher at 210°C , which was very near the crystalline melting point of nylon 6 (215°C). There is a chance that entanglements that tie crystalline blocks can slip out, and the ensuing viscous flow may lead to a change in crystal morphology.³³ Heat treatment at such a high temperature might have introduced

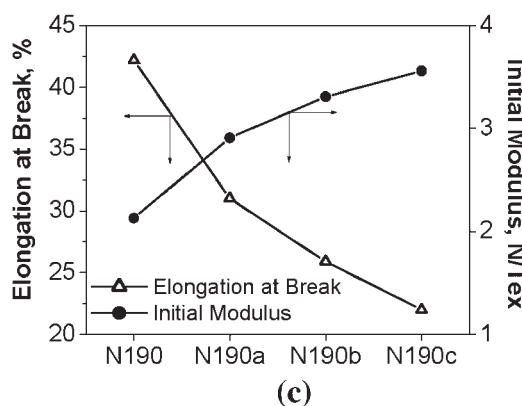
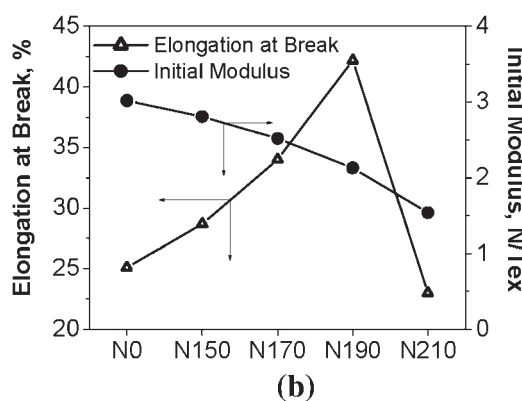
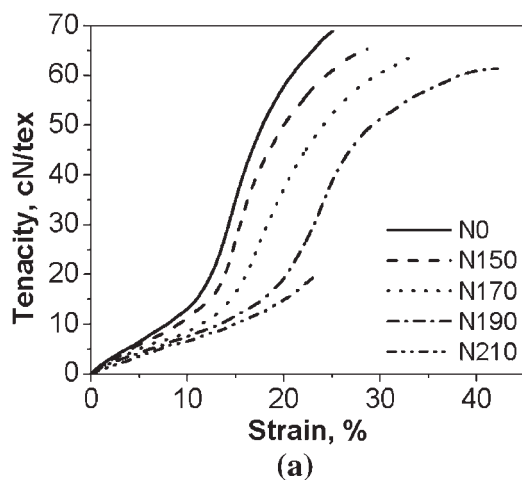


Figure 3 (a) Stress-strain plot of different heat-treated nylon 6 samples (freely shrunk), (b) elongation at break and initial modulus values for different heat-treated nylon 6 samples, and (c) elongation at break and initial modulus values for nylon 6 treated at 190°C under different loads.

some thermal degradation or chain folding, which led to a drastic reduction in strength. At any particular heat-treatment temperature, there was some change in the stress-strain properties with the change in applied stress (Fig. 4–6). When the applied stress was zero, that is, in conditions of free shrinkage, there was drop in tenacity and initial modulus but an increase in the elongation at break and energy of rupture compared with original untreated

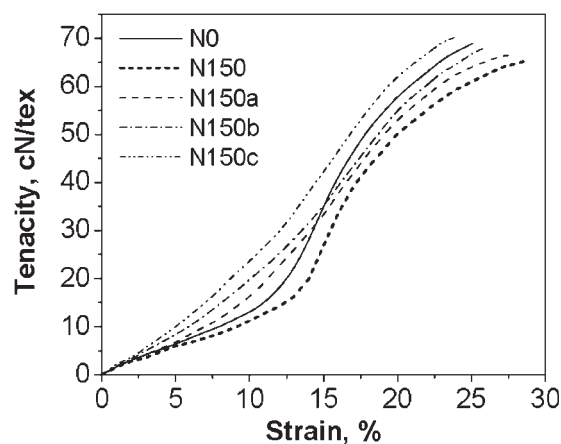


Figure 4 Stress-strain plot of nylon 6 treated at 150°C.

yarn. This difference between the untreated and treated yarn increased as the temperature of heat treatment increased. Figures 4–6 represent the stress-strain properties when heat treatment was carried out under a load at different temperatures. At higher applied stresses, there was an increase in the tenacity and initial modulus (Figs. 4–6) but a decrease in the elongation at break [Fig. 3(c)]. At any particular temperature, say at 190°C, with applied load changes, the variations in initial modulus and elongation at break are presented in Figure 3(c). The elongation at break continuously decreased with increasing applied load, whereas the initial modulus continuously increased.

Effect of the heat setting on the crystal structure

Because of the heat treatment, there was also some change in the nature of the DSC thermogram (Fig. 7). As clearly shown in Figure 7, there was increase in the sharpness of the DSC thermogram when the fiber was subjected to higher heat-treatment temperatures. There was also increase in the area under

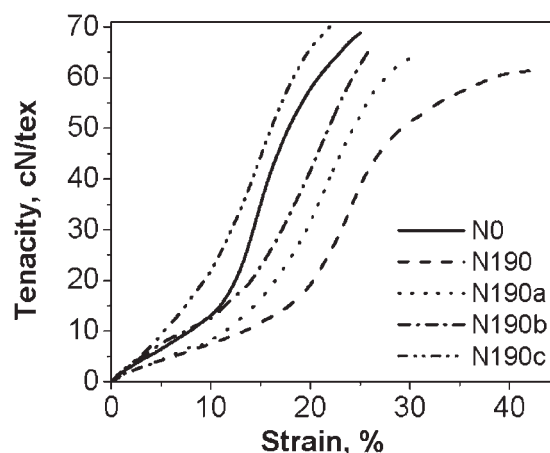


Figure 5 Stress-strain plot of nylon 6 treated at 190°C.

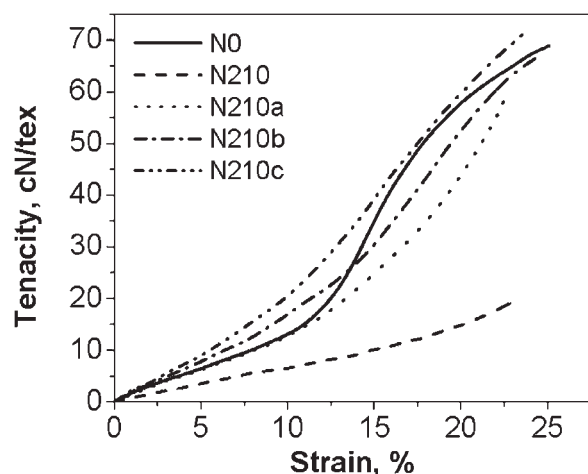


Figure 6 Stress-strain plot of nylon 6 treated at 210°C.

endotherm, which represented the heat of fusion and was proportional to crystallinity (Table III) or some ordering taking place in the fiber structure. A broad endotherm for the untreated yarn revealed that there existed crystals of different sizes in the nylon fiber. With heat treatment, there may have been changes in the crystal breadth along with its length. Also, there was some reorganization of some amorphous region within the two crystalline regions present in nylon cords. This organization of the amorphous region was reflected in the decrease in the elongation at break. However, the process of reorganization of crystalline and amorphous regions is temperature dependent. The rise in temperature affected in this organization process. Again, increasing heat-treatment temperature led to some kind of thermal organization in the crystal size distribution, which led to the melting of some small-size crystals and thus increased the density of bigger size crys-

tals. This was reflected in the sharpness of the endotherm and in the progressive shift of the main peak toward higher temperatures.

The XRD patterns of nylon 6 fibers subject to heat treatment at different temperatures are presented in Figure 8, and the details of different crystal parameters such as peak position, half width, d -spacing, and crystal size as calculated are presented in Table IV.

In Table IV, the average crystallite size was calculated with the Scherrer equation.³⁴ The average crystallite size increased with increasing heat-treatment temperature. Again, the half width for both major peaks showed a decreasing trend with increasing heat-treatment temperature. This reinforced the idea of either an increase in crystallinity or the perfection of crystal structures, which was also supported by the sharp DSC thermograms.

For the ease of distinguishing each individual X-ray, the plots were shifted by a constant factor along the Y axis. As shown in Figure 8, two major peaks were observed within 2θ values ranging from 20 to 25°. There was also a change in the peak position along with peak height and peak width (Table IV). For the untreated yarn, the first peak was observed at 21.6°, the second peak was observed at 23.4°, and the peaks were relatively broader. As per the literature, two types of crystal structures exist in nylon 6: α and γ .²⁰ The two intense reflections of the α and γ phases were at 21° (200, α_1) and 24° (002+202, α_2), and 22° (100, γ_1) and 23° (201+200, γ_2), respectively. That means these two peaks consisted of four different peaks merged together existing in different planes. The peak positions of these two peaks changed with different conditions of heat-treatment temperature. This revealed that there was a change in the relative proportion of the α and γ crystalline forms and spatial changes in the two types of crys-

TABLE II
Mechanical Properties of the Different Heat-Treated Samples

Sample	Breaking load (N)	Elongation at break (%)	Tenacity (cN/Text)	Initial modulus (cN/Text)	Work of rupture (N m)
N0	250.8	25.1	68.9	302.0	4.137
N150	238.3	28.7	65.3	281.0	4.788
N150a	242.4	27.5	66.4	296.0	4.887
N150b	248.6	26.0	68.1	320.0	4.618
N150c	256.2	23.9	70.2	341.0	4.440
N170	233.2	34.0	63.9	252.0	5.583
N170a	239.7	30.2	65.7	287.0	4.385
N170b	243.6	27.8	66.7	313	4.153
N170c	252.4	26.4	69.2	337	3.929
N190	223.7	42.2	61.3	213	6.844
N190a	236.1	31.0	64.7	291	4.432
N190b	239.4	25.9	65.6	331	3.588
N190c	255.8	22.0	70.1	356	3.790
N210	70.4	23.0	19.3	154	1.049
N210a	219.4	22.7	60.1	270	2.567
N210b	244.9	24.6	67.1	326	3.811
N210c	249.9	23.6	71.2	345	4.039

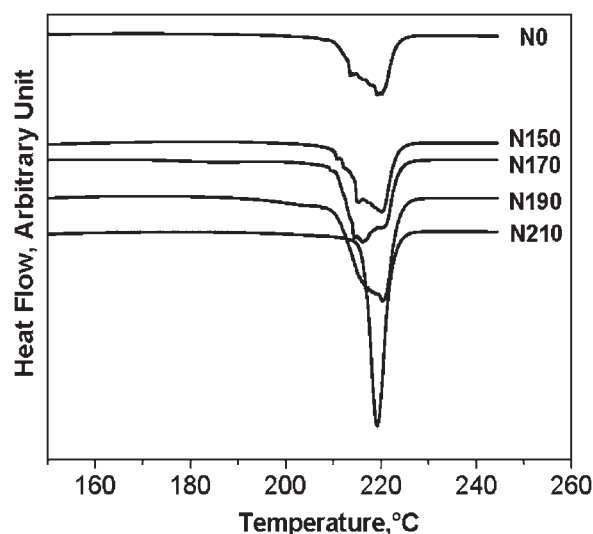


Figure 7 DSC thermograms of different heat-treated nylon 6 samples (freely shrunk).

tals.³⁵ Also, untreated nylon had both forms in different ratios, which led to some imperfection. However, on heat treatment, there was a reduction in one form with the increase in other form, which led to more perfection in the crystalline structure, which could be measured in terms of the crystal perfection index (CPI).³⁶

In general, XRD gives a better representation of crystallinity and crystalline structure for semicrystalline or highly crystalline polymers. However, it is worth mentioning here that the crystallinity measured for nylon 6 fiber in the usual procedure is not perfect.³⁷ It is mainly because the amorphous halo is buried inside the crystalline peaks and is not perfectly detectable. In such situation, CPI may be used to estimate the orderliness in highly oriented crystalline material.

CPI can be calculated with the following equation³⁸

$$\text{CPI} = \frac{(d_{200}/d_{002} - 1) \times 100}{0.1935} \quad (2)$$

where d_{200} is the interplanar spacing of (200) planes, d_{002} is the interplanar spacing of 002 planes, and 0.1935 is the corresponding value for a well-crystallized sample.

TABLE III
Crystallinity Calculated from the DSC
and XRD Analyses

Sample	Heat of fusion (J/g)	Crystallinity (%)	
		DSC	XRD
N0	80.4	42.0	56.0
N150	85.6	45.0	57.0
N170	89.3	47.0	60.0
N190	94.6	50.0	80.0
N210	105.9	56.0	91.0

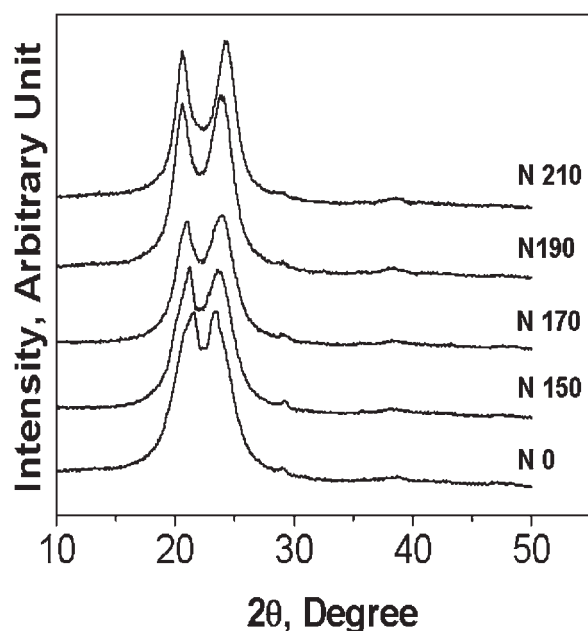


Figure 8 XRD of different heat-treated nylon 6 samples (freely shrunk).

CPI (%) at different heat-set temperatures is plotted in Figure 9. With increasing heat-treatment temperature, there was a progressive increase in CPI. As CPI increased, there was a change in the sharpness of the peak. Similarly, the crystalline perfection degree given in Table IV could also be correlated to the perfection of crystals, which was given by the difference of the peak positions of the two major peaks observed between 20 and 25°. The total crystallinity measured from X-ray analysis also increased progressively with heat-treatment temperature (Table III). Also, with changing tension, CPI generally increased (figure not shown).

It has been reported that there exists some relation between CPI measured from X-ray analysis and fiber density.³⁷ The density of the polymer again increased with increasing crystallinity. Even in fibers where there is a high degree of crystallinity due to orientation, there may exist some kinds of crystal defects. In fact, in a crystalline fiber, polymer chains run through successively crystalline and amorphous regions. However, this amorphous region present in the fiber is much more oriented and parallelized compared to the undrawn crystalline polymer. However, the level of organization present in the amorphous region of the fiber is not of that order that can be registered through X-ray. The heat-setting process often organizes this amorphous region and modifies the crystalline regions already present. Perhaps there may be some modification of crystallites and change in the shape and size of the crystallites.³⁹ There is also the possibility during heat setting that bigger

TABLE IV
Crystal Sizes and *d*-Spacings of Different Heat-Treated Samples

	Peak position (°)		<i>d</i> -spacing (Å)		Half-width (AU)		Crystal size (Å)		Crystalline perfection degree ^a
	First peak	Second peak	First peak	Second peak	First peak	Second peak	First peak	Second peak	
N0	21.6	23.4	4.111	3.799	1.7	2.18	48.0	37.0	1.8
N150	21.4	23.7	4.149	3.759	1.63	2.09	50.0	38.0	2.3
N170	21.3	23.9	4.169	3.728	1.52	2.01	53.0	40.0	2.6
N190	20.9	23.9	4.247	3.721	1.41	1.97	57.0	41.0	3.0
N210	20.6	24.2	4.309	3.675	1.32	1.93	61.0	43.0	3.6

^a Second peak – first peak (peak positions).

crystallites can become more perfect by expelling the defects out of the crystals.⁴⁰

The XRD patterns of fibers subjected to both thermal and mechanical stresses are given in Figure 10. Here, with the application of stress, the peak position of the measured peaks occurring within 20–25° changed marginally compared to those of the untreated and unset yarn. However, when some stress was applied on the yarn, some new crystalline peaks gradually appeared: one within 16.8–17° and two more peaks at 38.5; and 44.8°, respectively. This means that when both mechanical and thermal stresses were simultaneously applied on the fiber, there was a reorganization of crystalline structure. Perhaps there was also some organization of the relatively ordered amorphous region into crystalline form at different planes compared to the major crystalline forms occurring at planes 200 and 002.

Effect of the heat setting on the residual shrinkage

The residual heat shrinkage plays a very important role in determining the processing conditions of products such as tires and conveyor belts that use

nylon as the reinforcement. The residual heat shrinkage needs to be controlled for to attain the perfect size and shape of products derived from nylon. Hence, it is important to know the residual shrinkage of nylon cords, especially at vulcanization temperatures, when it is going to be used as rubber reinforcement. So, the residual shrinkage, measured at 150°C for both untreated and different heat-treated samples, is given in Table V. Compared to untreated samples, heat-treated samples always exhibited much lower residual shrinkage at 150°C. Cords that underwent free thermal shrinkage showed minimum residual shrinkage, and cords subjected to higher stress during heat treatment exhibited higher residual shrinkage in the latter stage of processing, that is, during curing. The residual shrinkage generally decreased with increasing heat-setting temperatures. This can be explained in terms of changes in chain folding and crystal imperfection present in the cord with changes in the heat-treatment temperature.^{31,40} The higher the heat-set temperature was, the higher the chance was of relaxation in locked-in stress generated during manufacturing that led to more stable

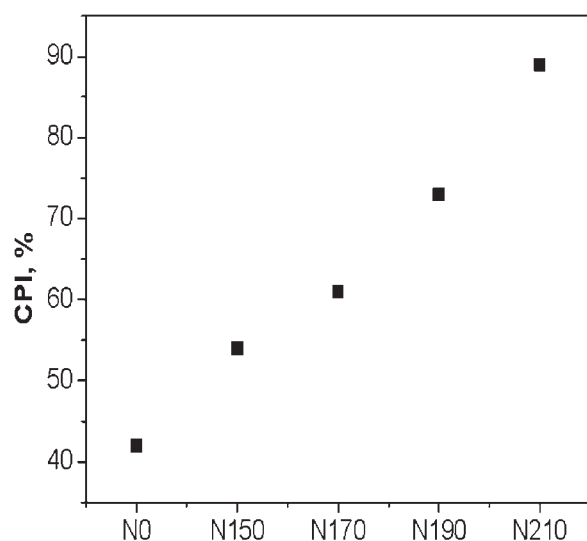


Figure 9 CPI values of different heat-treated nylon 6 samples (freely shrunk).

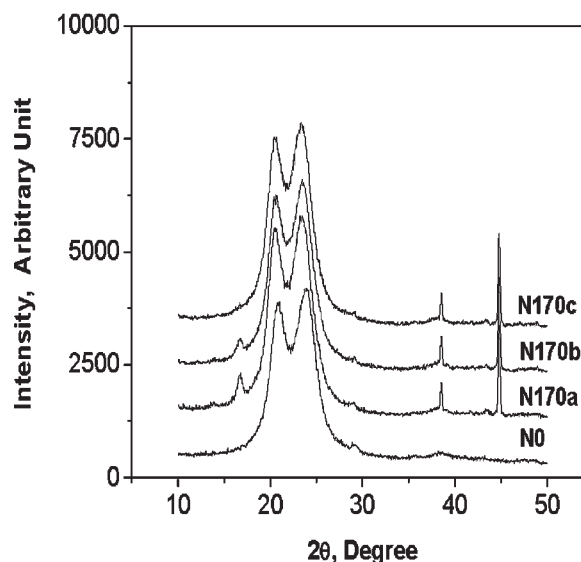


Figure 10 XRD of nylon 6 heat-treated at 170°C under different loads.

TABLE V
Residual Shrinkage at 150°C for Different Heat-Treated Samples

Heat-set temperature (°C)	Tension (N)	Residual shrinkage at 150°C (%)
150	0.00	3.5
	2.95	4.2
	4.40	4.7
	8.80	5.5
170	0.00	3.1
	2.95	3.5
	5.90	3.9
	8.80	4.6
190	0.00	2.6
	2.95	3.0
	6.27	3.5
	8.80	3.9
210	0.00	2.0
	2.95	2.7
	6.86	3.1
	8.80	3.5

structure and, hence, less residual shrinkage. This change in crystal structure due to heat treatment may have been more significant in changing the mechanical properties and the residual heat shrinkage.

CONCLUSIONS

Shrinkage force and the extent of shrinkage at different temperatures initially increased sharply with heat-treatment time and then attained some plateau within around 90 s.

In the case of free shrinkage, the tenacity decreased steadily with increasing heat-treatment temperature up to 190°C, and beyond this temperature, it decreased drastically. However, when the heat set was done under load, the tenacity again increased.

The elongation at break increased with increasing heat-treatment temperature up to 190°C and so did the work of rupture.

The initial modulus behaved in the same way as that of tenacity, which means in case of free shrinkage, the initial modulus decreased with increasing temperature, but when a load was applied, it increased with increasing load.

As the heat-set temperature increased, the residual shrinkage under the same load decreased, and with increasing load at a particular temperature, residual shrinkage increased. All of these changes could be correlated with changes in the crystal structure of the nylon 6 fiber.

There was an increase in the percentage crystallinity, CPI, and average crystal size with increasing heat-set temperature. The crystal *d*-spacing decreased with increasing heat-treatment temperature, and again, on heat setting, there was some change in the crystalline form.

References

- Chen, B. *Tire Sci Tech* 2004, 32, 2.
- Prevorsek, D. C.; Murthy, N. S.; Kwon, Y. D. *Rubber Chem Technol* 1987, 60, 659.
- Prevorsek, D. C.; Kwon, Y. D.; Sharma, R. K. *J Appl Polym Sci* 1980, 25, 2063.
- Prevorsek, D. C.; Beringer, C. W.; Kwon, Y. D. *Polym Mater Sci Eng* 1983, 49, 682.
- Takeyama, T.; Matsui, J.; Hijiri, M. In *Pneumatic Tire*; Clerk, S. K., Ed.; Washington, DC: U.S. Department of Transportation, 1981; Chapter 2, p 97.
- Wang, S.; Wang, J. *Polym Mater Sci Eng* 1988, 59, 1205.
- Ellison, M. S.; Zeronian, S. H.; Alger, K. W.; Aboul-Fadl, S. M.; Soler, T. M. *Polym Eng Sci* 1989, 29, 1738.
- Kwon, Y. D.; Prevorsek, D. C. *Kautsch Gummi Kunstst* 1985, 38, 21.
- Snyder, R. H. *J Appl Polym Sci* 1973, 17, 2003.
- Chakravarty, S. N.; Mustafi, S. K.; Rijhwani, H. K. *J Polym Mater* 1988, 5, 17.
- Wootton, D. B. *The Applications of Textiles in Rubber*; Rapra Technology: 2001.
- Ziabicki, A. *Fundamentals of Fiber Formation*; Wiley: London, UK, 1976; p 452.
- Tsuruta, M.; Koshimo, A. *J Appl Polym Sci* 1965, 9, 1.
- Tsuruta, M.; Koshimo, A. *J Appl Polym Sci* 1965, 9, 11.
- Tsuruta, M.; Koshimo, A. *J Appl Polym Sci* 1965, 9, 39.
- Koshimo, A. *J Appl Polym Sci* 1965, 9, 69.
- Koshimo, A.; Tagawa, T. *J Appl Polym Sci* 1965, 9, 117.
- Tsuruta, M.; Koshimo, A.; Shimoyama, T. *J Appl Polym Sci* 1965, 9, 129.
- Huisman, R.; Heuvel, H. M. *J Appl Polym Sci* 1989, 37, 595.
- Huisman, R.; Heuvel, H. M. *J Polym Sci Polym Phys Ed* 1976, 14, 921.
- Huisman, R.; Heuvel, H. M. *J Appl Polym Sci* 1978, 22, 2229.
- Murthy, N. S.; Bray, R. G.; Correale, S. T.; Moore, R. A. F. *Polymer* 1995, 36, 3863.
- Murthy, N. S.; Minor, H.; Latif, R. A. J. *Macromol Sci Phys* 1987, 26, 427.
- Murthy, N. S.; Minor, H. *Polym Commun* 1991, 32, 297.
- Murthy, N. S.; Reimschuessel, A. C.; Kramer, V. *J Appl Polym Sci* 1990, 40, 262.
- Dole, M. *J Polym Sci Part C: Polym Symp* 1967, 18, 57.
- Ringwaled, E. L.; Lawton, E. L. In *Polymer Handbook*; Bandrup, J.; Immergut, E. H., Eds.; Wiley: New York, 1975; p. V-73.
- Naskar, A. K.; Mukherjee, A. K.; Mukhopadhaya, R. *Polym Degrad Stab* 2004, 83, 173.
- Hearle, J. W. S. In *The Setting of Fibers and Fabrics*; Hearle, J. W. S.; Miles, L. W. C., Eds.; Mellow: Watford, England, 1971; p 1.
- Textile Reinforcement of Elastomers; Wake, W. C.; Wootton, D. B., Eds.; Applied Science: London, 1982; p 78.
- Mukherjee, A. K.; Gupta, B. D.; Sharma, P. K.; Uschold, R. E. *J Appl Polym Sci* 1984, 30, 4417.
- Murthy, N. S. *Polym Commun* 1991, 32, 301.
- Buckley, C. P.; Salem, D. R. *Polymer* 1987, 28, 69.
- Klug, H. P.; Alexandar, L. E. *X-Ray Diffraction Procedures for Polycrystalline and Amorphous Materials*; Wiley: New York, 1962.
- Parker, J. P.; Lindenmeyer, P. H. *J Appl Polym Sci* 1977, 21, 821.
- Dismore, P. F.; Statton, W. O. *J Polym Sci Part C: Polym Symp* 1966, 13, 133.
- Statton, W. O. *J Polym Sci Part C: Polym Symp* 1967, 13, 33.
- Huisman, R.; Heuvel, H. M. *J Polym Sci Phys Ed* 1976, 14, 941.
- Prevorsek, D. C.; Kwon, Y. D.; Sharma, R. K. *J Mater Sci* 1977, 12, 2310.
- Gupta, V. B. *J Appl Polym Sci* 2002, 83, 589.